

## Integrated Modeling and Variable Universe Fuzzy Control of a Hydrogen-Air Fuel Cell System

S. W. Tong<sup>1,\*</sup>, D. W. Qian<sup>2</sup>, J. J. Fang<sup>1</sup>, H. X. Li<sup>1</sup>

<sup>1</sup> College of Automation, Beijing Union University, Beijing 100101, P.R. China

<sup>2</sup> School of Control and Computer Engineering, North China Electric Power University, Beijing 102206, P.R. China

\*E-mail: [sun21st@sina.com](mailto:sun21st@sina.com)

*Received:* 9 January 2013 / *Accepted:* 8 February 2013 / *Published:* 1 March 2013

---

This paper deals with the problem of integrated modeling and control of a hydrogen-air fuel cell system with a DC-DC buck converter. Unlike hydrogen-oxygen fuel cells, the hydrogen-air fuel cell needs to consider the effect of the nitrogen and the water vapor to the system. Thus, the modeling of process becomes more complex. This paper focuses on a 1KW PEM fuel cell unit and develops the models of stack voltage, cathode flow, anode flow and DC-DC converter based on the mass conservation, Henry law, Dalton partial pressure law, ideal gas equation and electrochemical theory etc. According to the changes of the current of load and the polarization curve at the operational temperature, the stack output voltage can be controlled to a given value by using a variable universe fuzzy controller. Then a DC/DC buck converter is implemented to convert the stack output voltage to a standard 12V DC which can be used as a standard electric source for DC load.

---

**Keywords:** Fuel cell, Modeling, Fuzzy control, Variable universe, DC/DC buck converter.

### 1. INTRODUCTION

Hydrogen-air fuel cell as one of the promising kind of fuel cells has received great attention in recent years because of its low temperature, no pollution and easy operational mode [1]. It is a electricity generation device with low voltage and high current density. However, the stack output of the fuel cell is decided by the numbers of the cells in the stack and is usually not a standard voltage. A DC/DC converter [2] can be used to convert the stack output to a given value. Moreover, effective

control measurement must be taken to make the hydrogen-air fuel cell generate enough power for the load demands.

Many researchers have devoted themselves to the dynamic modeling and control of fuel cells [3]-[10]. Rodatz et al. [3] presented a dynamic model of the air supply of the fuel cell and applied an LQG regulator to the system. Vahidi et al. [4] studied the excessive oxygen starvation in fuel cell during high current demand and optimized the distribution of current demand between the fuel cell and the auxiliary source by using model predictive control. Chen et al. [5,6] modeled and analyzed the humidifier system and developed the feedback and feed-forward control algorithms to make sure the fuel cell maintaining its highest membrane water content under a wide range of operation conditions without flooding. Different control methods such as sliding mode control [7], adaptive control [8], fuzzy control [9] and neural network control [10] are implemented in the fuel cell system. In fact, the fuel cell is a nonlinear process. Nonlinear control methods like fuzzy control and neural network are more suitable to the control of the system. In this paper, we combine the variable universe idea with the real-time simplified fuzzy inference and improve the control performance of the fuel cell system. The variable universe idea was first proposed by Li [11]. It can use less control rules to achieve fine control [12]. This method has successfully been applied to the control of a quadruple inverted pendulum [13], the truck backer-upper system [14] and the wing rock phenomenon [15]. In this paper, we take our attentions on the integrated modeling and control of the whole system. We first model the stack voltage, the cathode flow, the anode flow and the DC/DC buck converter. Then we use a real-time simplified variable universe fuzzy control algorithm [16] that we proposed to realize the power control by taking the voltage as reference and the current of load as disturbance.

## 2. SYSTEM DESCRIPTION

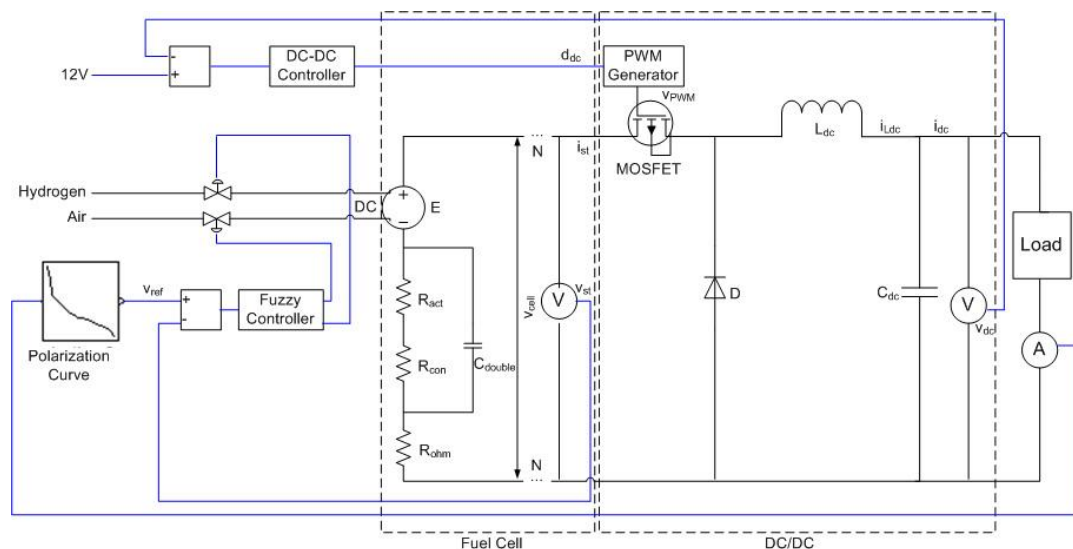


**Figure 1.** Power control scheme of the hydrogen-air fuel cell with DC/DC converter.

As Fig. 1 shown, our PEM fuel cell system, which has been designed and manufactured by the Institute of Automation of the Chinese Academy of Sciences (CASIA) and its industrial cooperator, is a 1KW electricity generation system. It uses hydrogen as fuel to take a chemical reaction with air. At the same time, byproduct water and heat have been produced. The stack of the fuel cell system has 24 cells in series and the active area of each cell is  $160\text{cm}^2$ . Output power of the stack is regulated by an air mass flow meter in the cathode inlet and a hydrogen mass flow meter in the anode inlet. The air mass flow meter is a kind of valve with 0–5V input voltage and 0–100SLM flow range, and the hydrogen mass flow meter is with 0–5V input voltage and 0–20SLM flow range. At the exit of the cathode and the anode channel, two hand valves whose opening are kept fixed in each experiment are equipped. The open voltage of the stack can come to 24V. However, our standard electric source of DC load is 12V. A DC/DC buck converter is used to convert the stack voltage to standard 12V.

### 3. SYSTEM MODEL

In modeling the fuel cell system model, we assume that the stack temperature has been controlled at  $65^\circ\text{C}$ , the relative humidify is constant and all gases are ideal gases. The PEM fuel cell system model is mainly composed of the stack voltage model, the cathode flow model, the anode flow model and the DC/DC converter model.

#### 3.1. Stack voltage model

The fuel cell stack consists of  $N$  cells in series. The stack voltage  $v_{st}$  can be easily obtained after calculating the voltage of a single cell  $v_{cell}$  by  $v_{st} = N \times v_{cell}$ . The basic expression for the voltage of a single cell [17] is:

$$v_{cell} = E - v_{act} - v_{ohm} - v_{con} \quad (1)$$

where the first term  $E$  on the right side of the equation is the reversible voltage [18]. It can be determined by

$$E = 1.229 - (8.5 \times 10^{-4})(T_{st} - 298.15) + 4.308 \times 10^{-5} T_{st} (\ln(P_{H_2}) + 0.5 \ln(P_{O_2})) \quad (2)$$

The second term  $v_{act}$  is the activation voltage that used to start the electrochemical reaction so as to make the reaction tend toward the formation of electricity and water, as opposed to the reverse [18]. It can be given by

$$v_{act} = a_1 + a_2 T_{st} + a_3 T_{st} \ln(i_{st}) + a_4 T_{st} \ln(c_{O_2}) \quad (3)$$

in which  $a_1, a_2, a_3, a_4$  are the identified parameters,  $c_{O_2} = P_{O_2} / (5.08 \times 10^6 \exp(-498/T_{st}))$ .

The third term  $v_{ohm}$  is the Ohmic voltage loss which is like the most common source of loss in any electrical device. This type of voltage loss results from the resistances of the conduction of protons through the solid electrolyte and the electrons through its path [19].

$$v_{ohm} = i_{st} \cdot R_{ohm} = i_{st} \cdot (R_{pro} + R_{ele}) \quad (4)$$

in which  $R_{ele}$  is the resistance to electron flow. It can be regarded as a constant.  $R_{pro}$  is the resistance to proton flow. It is determined by the following equations

$$R_{pro} = r_m \cdot \sigma_m / A$$

where  $r_m$  is the membrane specific resistivity for the flow of hydrated protons. The experimental equation for Nafion 112 ( $51 \mu m$ ) [19] is

$$r_m = \frac{181.6(1 + 0.03(\frac{i}{A}) + 0.062(\frac{T}{303})^2(\frac{i}{A})^{2.5})}{(\lambda - 0.634 - 3(\frac{i}{A}))\exp(4.18(\frac{T-303}{T}))}$$

The last term  $v_{con}$  represents the voltage losses resulting from the concentration reduction of the reactants gases or, alternatively, from the mass transport of the oxygen and the hydrogen.

$$v_{con} = B \cdot \ln(1 - \frac{i}{i_{max}}) \quad (5)$$

This paper also considers the charge double layer phenomenon [18] which reflects the dynamics of the fuel cell.

$$\frac{d(v_{act} + v_{con})}{dt} = \frac{i_{st}}{C_{double}} - \frac{v_{act} + v_{con}}{(R_{act} + R_{con})C_{double}} \quad (6)$$

where  $R_{act} = v_{act} / i_{st}$ ,  $R_{con} = v_{con} / i_{st}$ .

### 3.2. Cathode flow model

As Equations (2) and (3) shown, the gas partial pressure in the cathode affects the stack voltage of the fuel cell. We should well consider the gas partial pressure effect in the modeling of the cathode flow model. Applying the mass conversation principles, we have the equations (7)(8)(9).

$$\frac{dP_{O_2,ca}}{dt} = \frac{R T_{ca}}{V_{ca}} (F_{O_2,ca,in} - F_{O_2,rea} - F_{O_2,ca,out}) \quad (7)$$

$$\frac{dP_{N_2,ca}}{dt} = \frac{R T_{ca}}{V_{ca}} (F_{N_2,ca,in} - F_{N_2,ca,out}) \quad (8)$$

$$\frac{dP_{H_2O,ca}}{dt} = \frac{R T_{ca}}{V_{ca}} (F_{H_2O,ca,in} - k_{vap} F_{H_2O,gen} - F_{H_2O,ca,out}) \quad (9)$$

In our hydrogen-air fuel cell units, the input gas is the dry air which consists of 21%  $O_2$  and 79%  $N_2$ .

$$F_{O_2,ca,in} = f_{1,O_2} \cdot F_{air,in} = 0.21 F_{air,in}$$

$$F_{N_2,ca,in} = f_{1,N_2} \cdot F_{air,in} = 0.79 F_{air,in}$$

The dry air is humidified before entering the cathode channel. So the vapor form  $H_2O$  entering the cathode can be calculated with the following equation.

$$F_{H_2O,ca,in} = f_{1,H_2O} \cdot F_{air,in} = \frac{P_{H_2O,ca}}{P_{ca} - P_{H_2O,ca}} F_{air,in}$$

With the knowledge of thermodynamics of gas mixtures, the pressure of  $H_2O$  in the cathode is

$$P_{H_2O,ca} = \varphi_{ca} \cdot P_{sat}(T_{ca})$$

The  $O_2$  consumed and the  $H_2O$  generated in the chemical reaction can be obtained by using electrochemistry principles.

$$F_{O_2,rea} = \frac{Ni_{st}}{4F}$$

$$F_{H_2O,gen} = \frac{Ni_{st}}{2F}$$

The volume flow rate of the  $O_2$ ,  $N_2$  and the  $H_2O$  at the cathode exit can be given by a mole ratio of the total flow rate.

$$F_{O_2,ca,out} = f_{2,O_2} \cdot F_{ca,out} = \frac{P_{O_2,ca,out}}{P_{ca,out}} F_{ca,out}$$

$$F_{N_2,ca,out} = f_{2,N_2} \cdot F_{ca,out} = \frac{P_{N_2,ca,out}}{P_{ca,out}} F_{ca,out}$$

$$F_{H_2O,ca,out} = f_{2,H_2O} \cdot F_{ca,out} = \frac{P_{H_2O,ca,out}}{P_{ca,out}} F_{ca,out}$$

According to the mass conservation principles, the volume flow rate at the cathode exit has the following relation.

$$F_{ca,out} = F_{O_2,ca,out} + F_{N_2,ca,out} + F_{H_2O,ca,out}$$

Dalton partial pressure law can be applied to the cathode.

$$P_{ca} = P_{O_2,ca} + P_{N_2,ca} + P_{H_2O,ca}$$

Because the volume of the cathode channel is very small and the distance between the cathode exit valve and the stack is short, we can regard the pressure at the cathode exit valve equal to the total cathode pressure, i.e.  $P_{ca,out} = P_{ca}$ .

We use the following nonlinear function to describe the outlet mass flow rate of the cathode.

$$W_{ca,out} = a \cdot (-1 + \sqrt{1 + b \cdot (P_{ca} - P_{atm})})$$

where  $a, b$  are the identified parameters. The mass flow rate can be transformed into the volume flow rate by  $F_{ca,out} = k_{wf} W_{ca,out}$

As a summary of the above discussions, we have the following partial pressure equations.

$$\frac{dP_{O_2,ca}}{dt} = \frac{R T_{ca}}{V_{ca}} \left( 0.21 F_{air,in} - \frac{Ni_{st}}{4F} - \frac{P_{O_2,ca}}{P_{ca}} F_{ca,out} \right) \tag{10}$$

$$\frac{dP_{N_2,ca}}{dt} = \frac{R T_{ca}}{V_{ca}} \left( 0.79 F_{air,in} - \frac{P_{N_2,ca}}{P_{ca}} F_{ca,out} \right) \tag{11}$$

$$\frac{dP_{H_2O,ca}}{dt} = \frac{R T_{ca}}{V_{ca}} \left( \frac{\varphi_{ca} \cdot P_{sat}(T_{ca})}{P_{ca} - \varphi_{ca} \cdot P_{sat}(T_{ca})} F_{air,in} - k_{vap} \frac{Ni_{st}}{2F} - \frac{P_{H_2O,ca}}{P_{ca}} F_{ca,out} \right) \tag{12}$$

With a sum of Equations (10)(11) and (12), we can obtain the cathode pressure Equation (13).

$$\frac{dP_{ca}}{dt} = \frac{k_{wf} R T_{ca}}{V_{ca}} \left( \frac{\varphi_{ca} \cdot P_{sat}(T_{ca})}{P_{ca} - \varphi_{ca} \cdot P_{sat}(T_{ca})} W_{air,in} - \frac{Ni_{st}}{4F k_{wf}} + k_{vap} \frac{Ni_{st}}{2F k_{wf}} - a \cdot (-1 + \sqrt{1 + b \cdot (P_{ca} - P_{atm})}) \right) \quad (13)$$

### 3.3. Anode flow model

Similar to the inference of the cathode model, we can give the final partial pressure equations

$$\frac{dP_{H_2,an}}{dt} = \frac{R T_{an}}{V_{an}} \left( F_{H_2,an,in} - \frac{Ni_{st}}{2F} - \frac{P_{H_2,an,out}}{P_{an,out}} F_{an,out} \right) \quad (14)$$

$$\frac{dP_{H_2O,an}}{dt} = \frac{R T_{an}}{V_{an}} \left( \frac{\varphi_{an} \cdot P_{sat}(T_{an})}{P_{an} - \varphi_{an} \cdot P_{sat}(T_{an})} F_{H_2,in} - \frac{P_{H_2O,an,out}}{P_{an,out}} F_{an,out} \right) \quad (15)$$

and anode pressure equation

$$\frac{dP_{an}}{dt} = \frac{k_{wf} R T_{an}}{V_{an}} \left( \frac{P_{an}}{P_{an} - \varphi_{an} \cdot P_{sat}(T_{an})} W_{H_2,in} - \frac{Ni_{st}}{2F k_{wf}} - c \cdot (-1 + \sqrt{1 + d \cdot (P_{an} - P_{atm})}) \right) \quad (16)$$

### 3.4. DC/DC converter model

The DC/DC converter as Fig. 1 shown is a buck circuit. In our units, it is used to bring down the stack voltage to standard 12V DC. It consists of a MOSFET, an inductor, a diode and a capacitor. The output voltage of the DC/DC converter can be controlled by regulating the duty-ratio of the PWM generator. When  $v_{PWM} = 1$ , the diode is interrupted.

$$\begin{cases} \frac{di_{L_{dc}}}{dt} = \frac{1}{L_{dc}} v_{st} - \frac{1}{L_{dc}} v_{dc} \\ \frac{dv_{dc}}{dt} = \frac{1}{C_{dc}} i_{L_{dc}} - \frac{1}{C_{dc}} i_{dc} \end{cases} \quad (17)$$

When  $v_{PWM} = 0$ , the MOSFET is closed. Thus a close loop is formed between the diode, the inductor and the capacitor.

$$\begin{cases} \frac{di_{L_{dc}}}{dt} = -\frac{1}{L_{dc}} v_{dc} \\ \frac{dv_{dc}}{dt} = \frac{1}{C_{dc}} i_{L_{dc}} - \frac{1}{C_{dc}} i_{dc} \end{cases} \tag{18}$$

According to Equations (17) and (18), it can be calculated the output of any time of open or close of MOSFET by means of bounded condition. However, it will take hundreds of times to finish a regulation process. The calculation burden is very heavy. In fact, we can combine the two equations into a single equation by simply taking a linearly weighted average of the separate equations for each switched configuration of the converter.

$$\begin{cases} \frac{di_{L_{dc}}}{dt} = \frac{d_{dc}}{L_{dc}} v_{st} - \frac{1}{L_{dc}} v_{dc} \\ \frac{dv_{dc}}{dt} = \frac{1}{C_{dc}} i_{L_{dc}} - \frac{1}{C_{dc}} i_{dc} \end{cases} \tag{19}$$

#### 4. FUZZY CONTROLLER DESIGN

The inherent nonlinearity combined with the linguistic knowledge representation makes the fuzzy system a powerful tool in control. While PEM fuel cell is a nonlinear process, it is very suitable to use fuzzy control to solve the control issue of the fuel cell. Fuzzy inference methods have been implemented in the temperature [9] and power [20,21] control of the fuel cell system. However, there is often a conflict between the fine control and the real-time control. Well control needs to add more control rules thus increase the calculation burden. For example, Kisacikoglu et al. [20] integrate a fuel logic control algorithm into the power conditioning unit and they have used 80 fuzzy inference rules; Sakhare et al. [21] design a fuzzy controller of fuel cell for stand alone and grid connection and they have used 49 fuzzy inference rules. In this section, we propose a real-time simplified variable universe fuzzy control algorithm which can use 11 rules to achieve fine control by introducing the variable universe strategy.

##### 4.1. Initial universe and membership function

We adopt the typical structure with dual-inputs (error  $e$  and change in error  $ec$ ) and single output (control increment  $\Delta u$ ). The initial input universes of  $e$  and  $ec$  is  $X = [-E, +E]$  and  $Y = [-EC, +EC]$ , respectively, and output universe is  $Z = [-\Delta U, +\Delta U]$ .

The input  $e$  is adopted the triangular membership function as follows:

$$A^{-1}(x(k), k) = \begin{cases} 1, & x_1(k) \leq x(k) \leq x_2(k) \\ 1 - \frac{x(k) - x_2(k)}{x_3(k) - x_2(k)}, & x_2(k) \leq x(k) \leq x_3(k) \\ 0, & else \end{cases} \tag{20}$$

$$A^i(x(k), k) = \begin{cases} 1 + \frac{x(k) - x_i(k)}{x_i(k) - x_{i-1}(k)}, & x_{i-1}(k) \leq x(k) \leq x_i(k) \\ 1 - \frac{x(k) - x_i(k)}{x_{i+1}(k) - x_i(k)}, & x_i(k) \leq x(k) \leq x_{i+1}(k) \\ 0, & \text{else} \end{cases} \quad (21)$$

$$A^p(x(k), k) = \begin{cases} 0, & \text{else} \\ 1 + \frac{x(k) - x_{p-1}(k)}{x_{p-1}(k) - x_{p-2}(k)}, & x_{p-2}(k) \leq x(k) \leq x_{p-1}(k) \\ 1, & x_{p-1}(k) \leq x(k) \leq x_p(k) \end{cases} \quad (22)$$

where  $\{A^i\}_{(1 \leq i \leq p)}$  is a set of the linear basis elements of the initial universes  $X$ . Its peak points are  $\{x_i\}_{(1 \leq i \leq p+2)}$ , which satisfy  $-E = x_1 < x_2 < \dots < x_{p+2} = E$ .  $ec$  is also adopted a triangular membership function, which can be constructed the same way as  $e$ 's with linear basis elements  $\{B^j\}_{(1 \leq j \leq q)}$  whose peak points are  $\{y_j\}_{(1 \leq j \leq q+2)}$  satisfying  $-EC = y_1 < y_2 < \dots < y_{q+2} = EC$ .

It is assumed that the output universe has been divided into  $z_m(k), m = 1, 2, \dots, n$ , which satisfy  $-\Delta U = z_1 < z_2 < \dots < z_n = \Delta U$ , and a series of linguistic variables are connected with the output  $\Delta u$ . Then the membership function of output variable  $\Delta u$  can be described with a two-dimensional table form between the  $z_m(k)$  and the linguistic variables.

#### 4.2. Real-time simplified variable universe fuzzy logic inference

The real-time simplified variable universe fuzzy control has the following characteristics:

1) *Variable Universe*: The variable universe fuzzy control can use less control rules to achieve fine control performance by adjusting the input and output universes. The core idea is the universe contraction with the decreased error on the basis of the form of control rules keeping constant. The contraction of the universe is equivalent to increasing the control rules, thus it can improve the accuracy of control. Moreover, the design of variable universe fuzzy control does not need too much expert knowledge. Grasp of the rules trend by and large is enough. The universe changes can be achieved by multiplying flex factors of universes  $X, Y$  and  $Z$  defined as follows:

$$\alpha(x) = \left[ \frac{|x|}{E} \right]^{\tau_1}, 0 < \tau_1 < 1 \quad (23)$$

$$\beta(y) = \left[ \frac{|y|}{EC} \right]^{\tau_2}, 0 < \tau_2 < 1 \tag{24}$$

$$\gamma(x, y) = \left[ \left[ \frac{|x|}{E} \right]^{\tau_1} \right] \left[ \left[ \frac{|y|}{EC} \right]^{\tau_2} \right]^{\tau_3}, 0 < \tau_1, \tau_2, \tau_3 < 1 \tag{25}$$

2) *Real-time*: In our real-time simplified variable universe fuzzy control algorithm, we adopt triangular membership functions for inputs. From the characteristics of the designed triangular membership function, it can be seen that any input value can belong to at most two membership functions. Thus, for dual-inputs system, it can activate at most four control rules at a time. Moreover, the algorithm can be realized with C language based sfunctions. Therefore, the real-time inference algorithm can be implemented as an alternative of calculating all possible conditions in advance. This can simplify the controller design process.

3) *Simplicity*: The simplicity of the fuzzy control algorithm lies in not only the real-time inference itself but also the use of only several main control rules due to the introducing of the variable universe idea. The decrease of the calculation burden is the direct result of the simplicity. So as a return, it is very suitable for real-time control.

The input variables  $e$  and  $ec$  of a fuzzy controller can also be connected with a series of linguistic variables. Different linguistic variable pairs of  $e$  and  $ec$  determine different control output  $\Delta u$ . Then the linguistic variables of control output  $\Delta u$  can be referred as a two-dimensional table between the linguistic variables of  $e$  and  $ec$ .

Thus the real-time simplified variable universe fuzzy logic inference process can be concluded with the following steps:

*Step 0*: According to the arbitrary initial inputs  $x(0) \in X$ ,  $y(0) \in Y$  and the real-time fuzzy inference method calculate the output  $u(1)$ .

*Step k (k ≥ 1)*: Apply  $u(k)$  to the process, compare the process output with the reference input, it can obtain the controller input  $x(k)$ ,  $y(k)$ . Calculate  $x_i(k) = \alpha(x(k))x_i(0)$ ,  $y_j(k) = \beta(y(k))y_j(0)$ ,  $z_m(k) = \gamma(x(k), y(k))z_m(0)$ . Through the following real-time fuzzy inference method, calculate  $u(k+1)$ :

*Step INF<sub>1</sub>*:  $x(k)$  and  $y(k)$  are the input variables. Assume the membership functions belong to  $x(k)$  are  $A_k^i$  and  $A_k^{i+1}$ , and the membership functions belong to  $y(k)$  are  $B_k^j$  and  $B_k^{j+1}$ . They activate four control rules:  $C_k^{(i,j)}$ ,  $C_k^{(i,j+1)}$ ,  $C_k^{(i+1,j)}$ ,  $C_k^{(i+1,j+1)}$ .

*Step INF<sub>2</sub>*: Look up the control rules table, four corresponding linguistic terms of  $\Delta u(k+1)$  can be obtained. According to these linguistic terms, look up the membership function table of  $\Delta u(k+1)$ , four  $1 \times n$  membership matrices:  $M_k^1$ ,  $M_k^2$ ,  $M_k^3$  and  $M_k^4$  can be obtained.

*Step INF<sub>3</sub>*: Use the minimum method to calculate

$$\bar{M}_k^1(m) = \wedge(A_k^i, B_k^j, M_k^1(m)),$$

$$\bar{M}_k^2(m) = \wedge(A_k^i, B_k^{j+1}, M_k^2(m)),$$

$$\bar{M}_k^3(m) = \wedge(A_k^{i+1}, B_k^j, M_k^3(m)),$$

$$\bar{M}_k^4(m) = \wedge(A_k^{i+1}, B_k^{j+1}, M_k^4(m)),$$

where  $m = 1, 2, \dots, n$ .

Step *INF*<sub>4</sub>: Let  $\bar{\bar{M}}_k(m) = \vee(\bar{M}_k^1(m), \bar{M}_k^2(m), \bar{M}_k^3(m), \bar{M}_k^4(m))$ , where  $m = 1, 2, \dots, n$ , calculate the membership of the output variable using the maximum method.

Step *INF*<sub>5</sub>: The incremental control output  $\Delta u(k+1)$  is determined using the method of the center of gravity in Equation (26),

$$\Delta u(k+1) = \frac{\sum_{m=1}^n \bar{\bar{M}}_k(m) * z_m(k)}{\sum_{m=1}^n \bar{\bar{M}}_k(m)} \tag{26}$$

Step *INF*<sub>6</sub>: Calculate the control output  $u(k+1)$ ,

$$u(k+1) = u(k) + \Delta u(k+1) \tag{27}$$

### 4.3. Design of the fuzzy controller

The initial universes of input  $e$  and  $ec$  are assigned to  $[-2, +2]$ , and the universe of the output  $\Delta u$  is  $[-3, +3]$ . Note that the initial universes of  $e$  and  $ec$  may be different. The selection of initial universe is somewhat arbitrary because the input coverage can be regulated by scaling gains. In a general way, the initial universe is selected the symmetrical form.

Suppose  $e$  is a linguistic control input variable, a label set corresponding to  $e$  is as follows:

$$L(e) = \{NB, NS, ZE, PS, PB\}$$

where  $NB$ ,  $NS$ ,  $ZE$ ,  $PS$  and  $PB$  means negative big, negative small, zero, positive small and positive big, respectively. The membership function for the control input variable  $e$  is triangular with  $\{A^i\}_{(1 \leq i \leq 5)} = \{A^1, A^2, A^3, A^4, A^5\}$ ,  $\{x_i\}_{(1 \leq i \leq 7)} = \{-2, -4/3, -2/3, 0, +2/3, +4/3, +2\}$ . Any input value

can thus be a member of at most two sets, and the membership of each is a linear function of the input value.

The membership function of control input variable  $ec$  is constructed in the same way with  $\{B^j\}_{(1 \leq j \leq 7)} = \{B^1, B^2, B^3, B^4, B^5, B^6, B^7\}$ ,  $\{y_j\}_{(1 \leq j \leq 9)} = \{-2, -1.5, -1.0, -0.5, 0, +0.5, +1.0, +1.5, +2.0\}$ .

$$L(ec) = \{NB, NM, NS, ZE, PS, PM, PB\}$$

where  $NM$  and  $PM$  means negative middle and positive middle, respectively.

Considering the variable universe strategy, universe can contract with the decrease of the error. Under this mechanism, the partition of the error  $e$  becomes less important. So the linguistic variables corresponding to  $e$  can be used less than the  $ec$ 's.

To simplify the defuzzification process, the output membership function of  $\Delta u$  adopts the discrete form as Table 1 shown.

**Table 1.** Membership function of the output  $\Delta u$ .

$C(\Delta u)$	-3.0	-2.0	-1.0	0	1.0	2.0	3.0
NB	1.0	0.7	0.3	0	0	0	0
NM	0.7	1.0	0.7	0.3	0	0	0
NS	0.3	0.7	1.0	0.7	0.3	0	0
ZE	0	0.3	0.7	1.0	0.7	0.3	0
PS	0	0	0.3	0.7	1.0	0.7	0.3
PM	0	0	0	0.3	0.7	1.0	0.7
PB	0	0	0	0	0.3	0.7	1.0

Due to adopting variable universe idea, we can use less control rules to achieve fine control. In fact, the consideration of the control rules as Table 2 shown with bold face is good enough to control the process. Here is the regulating mechanism: At the start of the control program, the input  $e$  can be set to the region  $ZE$  by changing the scaling gain  $K_e$ . Then the variable universe strategy begins to work to keep the error  $e$  close to the region  $ZE$ . In this region, the regulation related to the variable  $ec$  is very valid. The input  $e$  sometimes may enter into the neighboring region. In this region, the control linguistic variable is  $ZE$ . However, due to the overlap of the input membership function between  $ZE$  and its adjacent region  $NS$  or  $PS$ , the output of the control is not equal to zero. The input  $e$  can be pulled back to the region  $ZE$  under the negative feedback mechanism. After several control cycles, the control object can be achieved.

**Table 2.** Map of the control rules.

$\Delta u$	$e$					
	NB	NS	ZE	PS	PB	
$ec$	NB	ZE	ZE	<b>NB</b>	ZE	ZE
	NM	ZE	ZE	<b>NM</b>	ZE	ZE
	NS	ZE	ZE	<b>NS</b>	ZE	ZE
	ZE	<b>NBNS</b>	<b>ZE</b>	<b>PS</b>	<b>PB</b>	
	PS	ZE	ZE	<b>PS</b>	ZE	ZE
	PM	ZE	ZE	<b>PM</b>	ZE	ZE
	PB	ZE	ZE	<b>PB</b>	ZE	ZE

### 5. SIMULATION RESULTS

To simulate the whole fuel cell system with a DC/DC converter, we build up the models in the Matlab’s Simulink environment. Fig. 2 shows the simulation blocks in Simulink. It mainly consists of three subsystems: the fuel cell, the DC/DC converter and the flow controller. Details of the models are shown in Fig. 3-Fig. 5. The ‘fuel cell’ subsystem takes hydrogen mass flow meter set-point voltage and the air flow meter set-point voltage as input and gives stack voltage as output. The load current can be regarded as a disturbance input, which changes the output voltage. This subsystem contains different blocks to represent related mathematical models. The ‘DC/DC converter’ subsystem is used to convert the stack output voltage to a standard 12V DC by a DC/DC controller with the following form of transfer function:

$$\frac{1.8(s + 100)(s + 100)}{s(s + 6000)}$$

The ‘flow controller’ subsystem uses a real-time simplified variable universe fuzzy controller to regulate the flow of hydrogen and the air depending on the stack output voltage, in which the air flow is proportional to the hydrogen flow. The reference stack output voltage is calculated by the polarization curve at 65 °C which takes the load current disturbance as input. The variable universe fuzzy controller algorithm is realized using C-Sfunctions. Fig. 6 displays the simulation results. In this simulation, the controller parameters are set as follows. The scale factors  $K_e$ ,  $K_{ec}$ ,  $K_u$  are 0.05, 0.084 and 0.3. The parameters  $\tau_1$ ,  $\tau_2$ ,  $\tau_3$  related to the flex factors are assigned by 0.2, 0.15 and 0.01. It can be seen that the stack voltage has been controlled to a given value and the DC/DC converter output voltage has been controlled to a standard 12V. To testify the control performance, we compare the variable universe fuzzy control method with the ordinary fuzzy control approach as shown in Fig. 7. The design process of the ordinary fuzzy control algorithm can be obtained in [9,20,21]. In fact the ordinary fuzzy controller can be seen as a special case of the variable universe fuzzy controller that the

universe is kept fixing. In this section, all the flex factors of universes  $X$ ,  $Y$  and  $Z$  are set to 1 to simulate an ordinary fuzzy controller. From the response before 40 seconds in Fig. 7, it can not be clearly seen if the performance of the variable universe fuzzy control is better than the ordinary fuzzy control because the universe is rough at this time. Then the variable universe mechanism begins to work. The universe contracts with the decrease of the error. The response under the variable universe fuzzy control becomes better than the ordinary fuzzy control. The simulation results demonstrate that the variable universe fuzzy control is very effective.

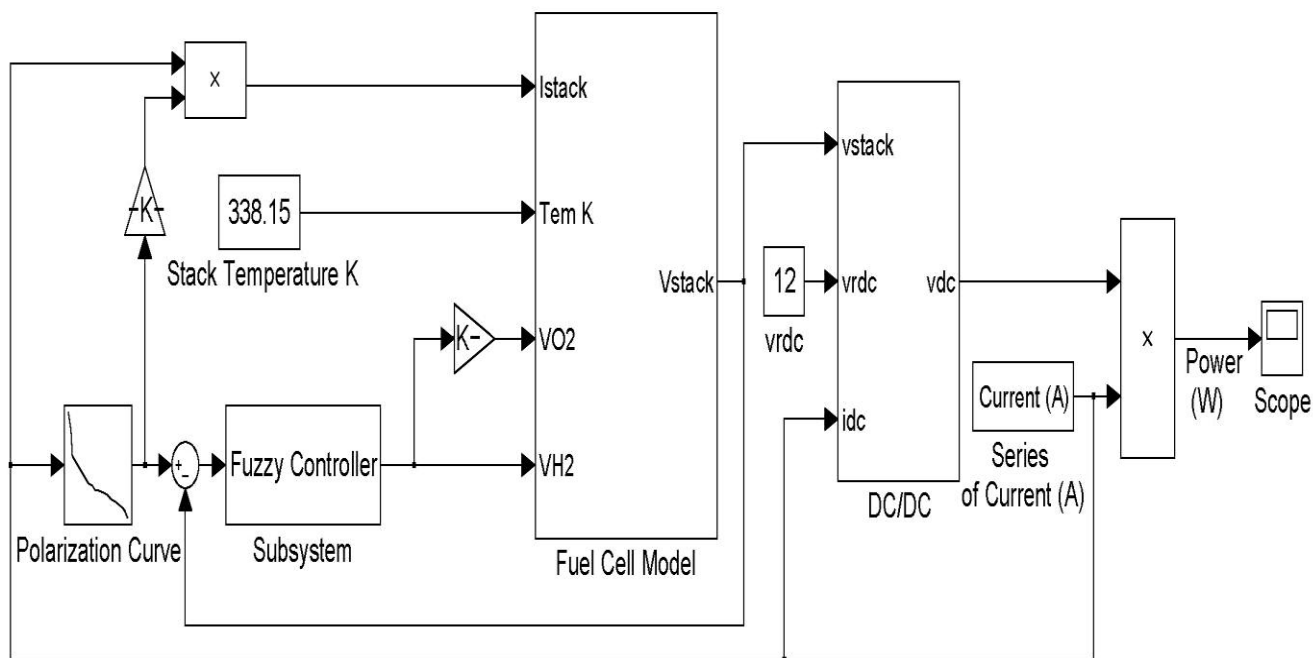


Figure 2. Simulink diagram of the power control of the hydrogen-air fuel cell with DC/DC converter.

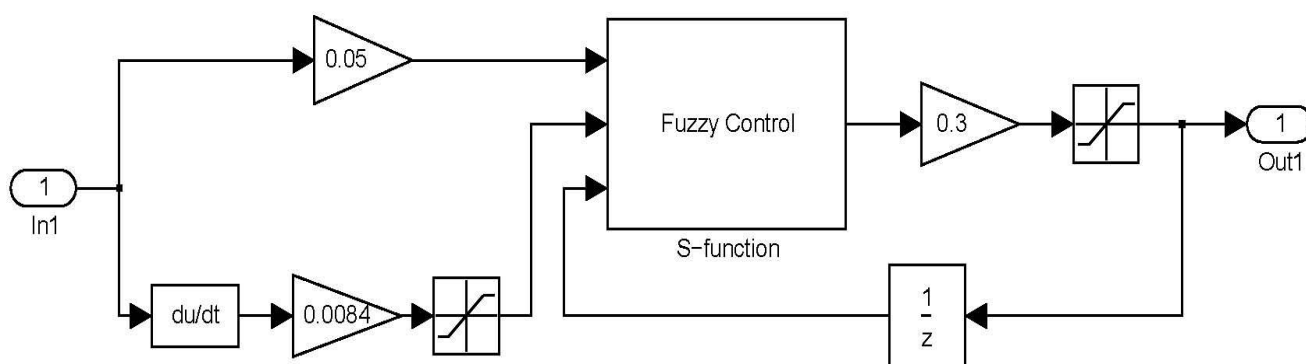


Figure 3. Simulink diagram of the real-time simplified variable universe fuzzy controller.

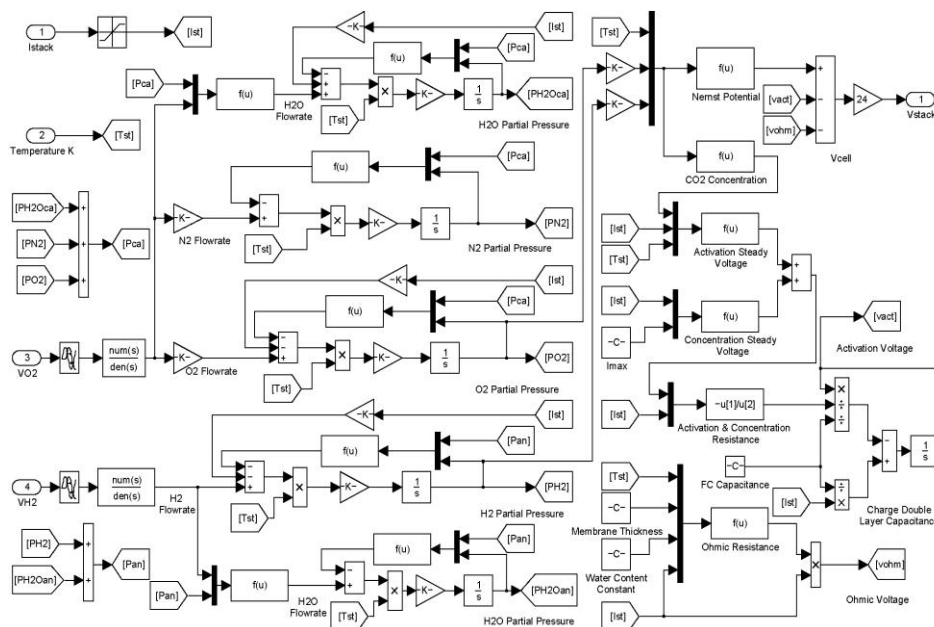


Figure 4. Simulink diagram of the hydrogen-air PEM fuel cell model.

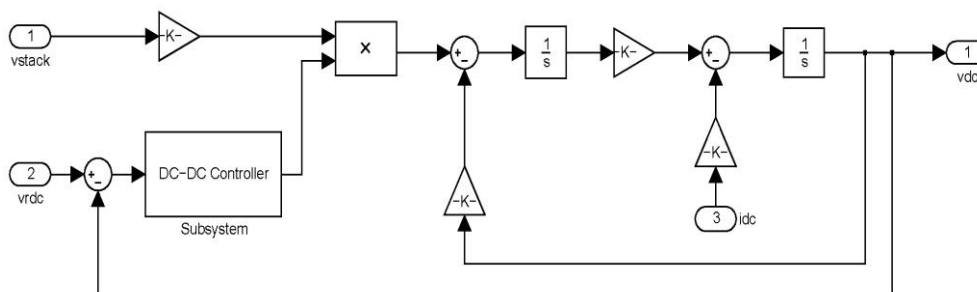


Figure 5. Simulink diagram of the model and controller of the DC/DC converter.

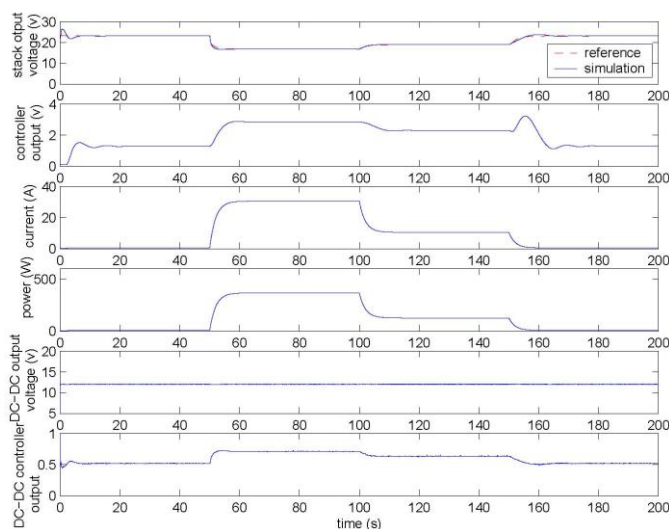
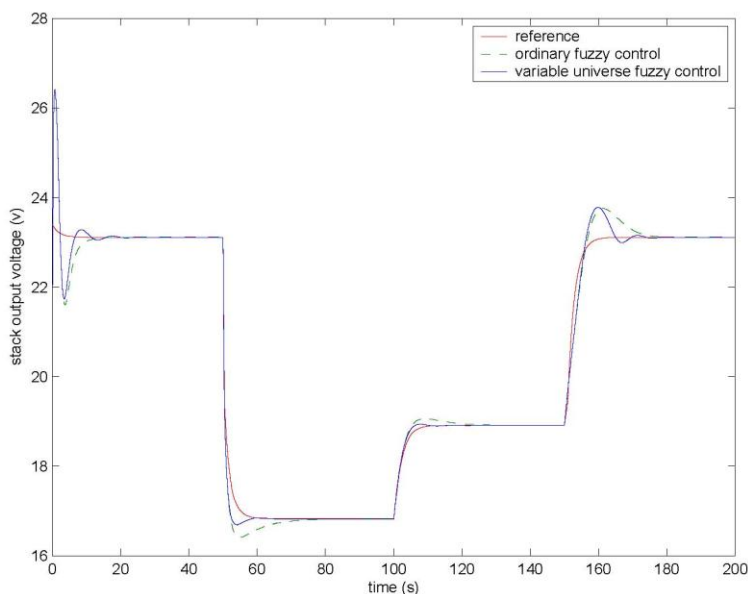


Figure 6. Simulative results.



**Figure 7.** Performance comparison between the variable universe fuzzy control and the ordinary fuzzy control.

## 6. CONCLUSIONS

This paper has built up the dynamic models, which include the stack voltage model, the cathode flow model, the anode flow model and the DC/DC buck converter model, of a 1KW hydrogen-air fuel cell system. By introducing a DC/DC controller, the stack output voltage can be converted to standard 12V DC. Thus, the power demand of the external load can be provided by the fuel cell stack under the control of a real-time simplified variable universe fuzzy controller.

## ACKNOWLEDGEMENTS

This work was supported by the New Start Program of the Beijing Union University under grant No. ZK20120016, Natural Science Foundation of Hebei Province under grant No. F2012502023, and the Fundamental Research Funds for the Central Universities under grant No. 12TD02.

## References

1. J.M. Corrêa, F.A. Farret, L.N. Canha, M.G. Simões, *IEEE Transactions on Industrial Electronics*, 51(2004)1103-1112.
2. S.Y. Choe, J. G. Lee, J. W. Ahn, S. H. Baek, *Journal of Power Sources*, 164(2007)614-623.
3. P. Rodatz, G. Paganelli, L. Guzzella, in: *Proceeding of the American Control Conference*, (2003)2043-2048.
4. A. Vahidi, A.G. Stefanopoulou, H. Peng, in: *Proceeding of the American Control Conference*, (2004)834-839.

5. D.M. Chen, H. Peng, in: *Proceeding of the American Control Conference*, (2004)822-827.
6. D.M. Chen, H. Peng, in: *Proceeding of the American Control Conference*, (2005)3853-3858.
7. G. Park, Z. Gajic, *Journal of Power Sources*, 212(2012)226-232.
8. Y. P. Yang, Z. W. Liu, F. C. Wang, *Journal of Power Sources*, 179(2008)618-630.
9. P. Hua, G. Y. Cao, X. J. Zhu, M. Hu, *International Journal of Hydrogen Energy*, 35(2010)9110-9123.
10. P.E.M. Almeida, M.G. Simões, *IEEE Transactions on Industry Applications*, 41(2005)237-245.
11. H.X. Li, *Fuzzy Systems and Mathematics*, 9(1995)1-14.
12. H.X. Li, *Science in China (Series E)*, 20(1999)32-42.
13. H.X. Li, Z.H. Miao, J.Y. Wang, *Science in China (Series E)*, 45(2002)213-224.
14. X.Y. Yang, Q.X. You, H.X. Li, *Journal of Beijing Normal University (Natural Science)*, 41(2005)348-350.
15. Z.L. Liu, C.Y. Su, J. Svoboda, in: *Proceeding of the American Control Conference*, (2004)1719-1724.
16. S.W. Tong, G.P. Liu, *European Journal of Control*, 14(2008)223-233.
17. J.T. Pukrushpan, A.G. Stefanopoulou, H. Peng, in: *Proceedings of the American Control Conference*, (2003)3117-3122.
18. M.J. Khan, M.T. Iqbal, *Renewable Energy*, 30(2005)421-439.
19. R.F. Mann, J.C. Amphlett, M.A.I. Hooper, H.M. Jensen, B.A. Peppley, P.R. Roberge, *Journal of Power Sources*, 86(2000)173-180.
20. M.C. Kisacikoglu, M. Uzunoglu, M.S. Alam, *International Journal of Hydrogen Energy*, 34(2009)1497-1507.
21. A. Sakhare, A. Davari, A. Feliachi, *Journal of Power Sources*, 135(2004)165-176.